

MIRAGE: Knowledge Graph-Guided Cross-Cohort MRI Synthesis for Alzheimer’s Disease Prediction

Guanchen Wu¹, Zhe Huang², Yuzhang Xie¹, Runze Yan¹, Akul Chopra¹,
Deqiang Qiu¹, Xiao Hu¹, Fei Wang², and Carl Yang¹✉

¹ Emory University, Atlanta, USA

² Cornell University, New York, USA

j.carlyang@emory.edu

Abstract. Reliable Alzheimer’s disease (AD) diagnosis increasingly relies on multimodal assessments combining structural Magnetic Resonance Imaging (MRI) and Electronic Health Records (EHR). However, deploying these models is bottlenecked by modality missingness, as MRI scans are expensive and frequently unavailable in many patient cohorts. Furthermore, synthesizing de novo 3D anatomical scans from sparse, high-dimensional tabular records is technically challenging and poses severe clinical risks. To address this, we introduce MIRAGE, a novel framework that reframes the missing-MRI problem as an anatomy-guided cross-modal latent distillation task. First, MIRAGE leverages a Biomedical Knowledge Graph (KG) and Graph Attention Networks to map heterogeneous EHR variables into a unified embedding space that can be propagated from cohorts with real MRIs to cohorts without them. To bridge the semantic gap and enforce physical spatial awareness, we employ a frozen pre-trained 3D U-Net decoder strictly as an auxiliary regularization engine. Supported by a novel cohort-aggregated skip feature compensation strategy, this decoder acts as a rigorous structural penalty, forcing 1D latent representations to encode biologically plausible, macro-level pathological semantics. By exclusively utilizing this distilled “diagnostic-surrogate” representation during inference, MIRAGE completely bypasses computationally expensive 3D voxel reconstruction. Experiments demonstrate that our framework successfully bridges the missing-modality gap, improving the AD classification rate by 13% compared to unimodal baselines in cohorts without real MRIs. ³

Keywords: MRI Synthesis · Knowledge Graph · Feature Engineering.

1 Introduction

Alzheimer’s disease (AD) is a progressive neurodegenerative disorder requiring early diagnosis for effective intervention [1]. In clinical practice, reliable AD diagnosis relies on comprehensive assessment combining structural neuroimaging,

³ The implementation details and codes are available in the anonymous repository at <https://anonymous.4open.science/r/MIRAGE-71B6>.

such as Magnetic Resonance Imaging (MRI), and Electronic Health Records (EHR)[5,6]. These data sources provide complementary value: MRI identifies structural biomarkers such as hippocampal atrophy, while EHR captures clinical trajectories including cognitive assessments, medical history, and demographics [17,26,28]. Recognizing this synergy, state-of-the-art machine learning models for AD classification increasingly employ multimodal architectures [17,16]. By jointly leveraging EHR and MRI, models achieve higher reliability and accuracy than unimodal approaches, establishing a new standard for AD analysis.

However, fundamental modality imbalance limits real-world multimodal model deployment [27,11]. Although EHR is routinely collected and accessible, expensive and clinically complex MRI acquisition [14,4] causes frequent missing scans in large cohorts. Because patients with and without MRI frequently originate from partially overlapping or institution-specific cohorts under varying protocols, this missing-modality challenge becomes a cross-cohort knowledge transfer problem where MRI-rich cohorts structurally guide EHR-only ones. Here, EHR-only patients combine clinical records with transferred structural guidance to generate MRI representations. Synthesizing patient-specific 3D MRIs from tabular records is a natural but ill-posed solution: generating anatomically faithful voxel-level scans from low-dimensional EHR remains challenging and clinically risky [3,29]. Crucially, downstream diagnostic models require MRI-encoded structural priors and latent disease manifolds rather than visually perfect images. Therefore, we reformulate the problem as anatomy-guided cross-modal distillation. Instead of reconstructing full MRI volumes at inference, we project EHR into a structurally grounded latent space to activate MRI-derived priors directly in feature space, avoiding expensive, artifact-prone voxel reconstruction.

Extracting a diagnostic-quality structural surrogate from EHR without empirical neuroimaging faces three challenges: (i) *EHR Sparsity and Heterogeneity*: Raw electronic health records are high-dimensional, sparse, and affected by schema variation across institutions. Direct reliance on this data obscures neurodegenerative states and confounds representation learning; (ii) *The Cross-Modal Semantic Gap*: Direct mapping from sparse, unstructured clinical features to a complex 3D imaging distribution often leads to posterior collapse and fails to capture structural priors; (iii) *Lack of Anatomical Constraints*: Standard cross-modal mappings lack spatial awareness. Projecting clinical data into an imaging manifold without explicit structural bounds yields biologically implausible latent representations, reducing prognostic value for AD.

To address these challenges, we introduce MIRAGE, a cross-cohort inference framework transferring MRI-derived structural knowledge from imaging-rich to EHR-only cohorts. MIRAGE decouples learning into graph-guided semantic propagation and anatomy-constrained joint optimization. To overcome EHR sparsity, Biomedical Knowledge Graphs (KGs) [7,10,21,24] and a Graph Attention Network (GAT) [20,2] map diverse clinical variables to a unified semantic space, inferring missing contexts from data-rich nodes. To bridge semantic gaps and enforce spatial awareness, a pre-trained 3D U-Net decoder serves as an auxiliary regularization engine. During training, an adapter maps EHR em-

beddings into MRI latent space. To satisfy the frozen 3D decoder’s requirement for high-frequency details, we introduce Cohort-Aggregated Skip Feature Compensation. By retrieving spatial priors (skip connections) from top- K clinically analogous patients, the decoder reconstructs pseudo-3D MRIs to compute voxel-level penalties (e.g., SSIM [22]). Rather than synthesizing exact patient anatomy, this reconstruction acts as a structural penalty forcing 1D latent representations to encode macro-level pathological semantics. Discarding this heavy 3D generative branch during inference, a classification head processes the distilled 1D latent vector, enabling efficient and accurate AD screening for EHR-only patients.

To the best of our knowledge, MIRAGE is the first framework to cast the missing-MRI problem as an anatomy-guided latent distillation task using a frozen 3D autoencoder as a structural regularizer. Our contributions are summarized as follows: (i) An Anatomy-Guided Cross-Modal Distillation framework that refines EHR representations through latent regularization, showing that structural priors improve AD diagnosis without pixel-level synthesis. (ii) A KG-Driven Cohort Alignment mechanism that addresses inconsistent EHR schemas by linking heterogeneous cohorts into a unified, semantically dense graph. (iii) An Auxiliary Decoding Regularization strategy that leverages cohort-retrieved skip features to bridge macro-prognostic representations and micro-texture constraints of a 3D MRI decoder. (iv) Clinical validation demonstrating that the framework bridges the missing-modality gap, improving the AD classification rate by 13% over unimodal baselines while maintaining high inference efficiency.

2 Method

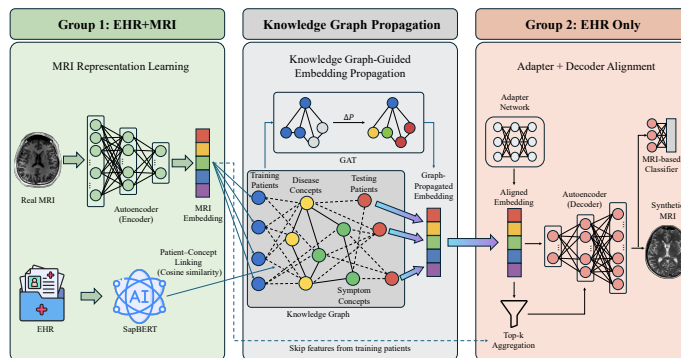


Fig. 1: Overall framework of MIRAGE.

Problem Formulation and Framework Overview. Let $KG = (X, R, RT)$ be a heterogeneous biomedical knowledge graph, where nodes $X = \mathcal{P} \cup \mathcal{T} \cup \mathcal{M}$ denote training patients, testing patients, and medical concepts. For each $i \in$

\mathcal{P}_{tr} , we observe a 3D MRI scan $X_i \in \mathbb{R}^{H \times W \times D}$ and label y_i . For $j \in \mathcal{P}_{te}$, only EHR features are available. The objective is to synthesize an MRI volume \hat{X}_j preserving anatomical realism and diagnostic utility for downstream classification. To bridge the modality gap for patients without neuroimaging, we propose MIRAGE (MRI Inference and Reconstruction via Aligned Graph-guided Embeddings). The framework integrates representation learning, graph-based propagation, and generative decoding. As shown in Figure 1, it operates in three phases. First, a 3D autoencoder maps real MRIs to a compact latent space. Second, a GAT propagates these representations over the biomedical knowledge graph to estimate latent embeddings for EHR-only patients. Finally, Adapter+Decoder alignment refines these embeddings and reconstructs synthetic MRI volumes while optimizing diagnostic utility.

MRI Representation Learning. The framework learns a compact latent representation of neurological structures using a 3D U-Net autoencoder (AE) with encoder f_{enc} and decoder f_{dec} , trained on patients with real neuroimaging data: $X_i \in \mathbb{R}^{1 \times H \times W \times D} : i \in \mathcal{P}_{tr}$. The encoder f_{enc} compresses input X_i into a latent manifold $z_i \in \mathbb{R}^d$ and extracts hierarchical spatial features $skip_i = skip_i^{(1)}, \dots, skip_i^{(4)}$. The decoder f_{dec} uses the latent vector and skip connections to reconstruct the volume:

$$z_i = f_{enc}(X_i), \quad \hat{X}_i = f_{dec}(z_i, skip_i). \quad (1)$$

Skip connections preserve high-frequency anatomical details. The autoencoder minimizes voxel-level mean squared error (MSE):

$$\mathcal{L}_{AE} = \frac{1}{|\mathcal{P}_{tr}|} \sum_{i \in \mathcal{P}_{tr}} |f_{dec}(f_{enc}(X_i), skip_i) - X_i|^2. \quad (2)$$

After convergence, decoder weights f_{dec} are frozen and used as the generative engine for MRI synthesis in later stages.

KG-Guided Embedding Propagation. With the MRI latent space established, the next step is to infer latent representations for testing patients with only EHR data. We formulate this as embedding propagation over a heterogeneous biomedical knowledge graph.

(I) Patient-to-KG Linking via EHR Concepts. We use a medical knowledge graph with concept nodes \mathcal{M} representing clinical ontology. Each patient $p \in \mathcal{P}_{tr} \cup \mathcal{P}_{te}$ is added as a node. Edges between patients and concepts are created using SapBERT [15,25,23], which generates 768-D embeddings for EHR concept descriptions and KG nodes. Cosine similarity connects patient nodes to concept nodes, grounding clinical profiles in the biomedical ontology.

(II) Two-Stage GAT Training. Node features $x^{(0)}$ are initialized as z_i for $x \in \mathcal{P}_{tr}$, g_x for $x \in \mathcal{M}$, and $\mathbf{0}$ for $x \in \mathcal{P}_{te}$. Because features lie in heterogeneous spaces, node-type-specific linear layers project them into a shared d -dimensional space: $h_x^{(0)} = W_{\tau(x)}x^{(0)} + b_{\tau(x)}$. Testing patients initially contain no internal

features and rely on aggregation from linked concept nodes. We apply a three-layer GATv2 [2] with residual connections for attention-weighted aggregation: $x^{(\ell+1)} = \text{GATv2}(x^{(\ell)}, \mathcal{E})$. Training proceeds in two stages.

Stage 1: Supervised Regression. The network first regresses ground-truth MRI latent vectors (z_i):

$$\mathcal{L}_{\text{GCN}} = \sum_{i \in \mathcal{P}_{\text{tr}}} \|h_i^{(L)} - z_i\|^2. \quad (3)$$

Stage 2: Decoder-Consistency Fine-Tuning. To ensure compatibility with the frozen AE decoder, GAT outputs $h_i^{(L)}$ are decoded and penalized for reconstruction errors using SSIM:

$$\mathcal{L}_{\text{recon_GAT}} = \|f_{\text{dec}}(h_i^{(L)}) - X_i\|^2 + (1 - \text{SSIM}(f_{\text{dec}}(h_i^{(L)}), X_i)). \quad (4)$$

After this optimization, the GAT infers synthetic embeddings $u_j = h_j^{(L)}$ for all testing patients $j \in \mathcal{P}_{\text{te}}$.

Adapter and Decoder Alignment. Although GAT provides strong latent approximations, distributional shifts degrade MRI synthesis. We introduce a trainable adapter and classification head optimized with the frozen decoder.

(I) WC Transformer. Before adaptation, we align graph-propagated embeddings (u_i) with the AE latent space using a Whitening-Coloring (WC) transformation [13]. Using means (μ_u, μ_z) and covariance matrices (Σ_u, Σ_z), we obtain the aligned embedding \tilde{u}_i :

$$\tilde{u}_i = \Sigma_z^{1/2} \Sigma_u^{-1/2} (u_i - \mu_u) + \mu_z$$

This alignment improves decoding stability and synthesis quality for the decoder.

(II) Adapter Network and Skip Feature Aggregation. The adapter A_θ maps GAT embeddings u_j into the decoder space: $\tilde{z}_j = A_\theta(u_j)$. High-resolution decoding also requires spatial skip features missing for testing patients. We address this with top- K nearest-neighbor aggregation. For embedding u_j , the K most similar training patients are selected via cosine similarity. Their skip features are aggregated using normalized similarity weights:

$$\hat{s}_j^{(k)} = \sum_{i \in \mathcal{N}_K(j)} w_i s_i^{(k)}, \quad \text{where } w_i = \frac{\max(\cos(u_j, z_i), 0)}{\sum_{m \in \mathcal{N}_K(j)} \max(\cos(u_j, z_m), 0)}. \quad (5)$$

For efficiency, we use $K = 1$ to supply spatial priors.

(III) Joint Objective Optimization. During inference, the synthetic MRI is generated as: $\hat{X}_j = f_{\text{dec}}(\tilde{z}_j, \hat{s}_j^{(1)}, \dots, \hat{s}_j^{(4)})$. To ensure anatomical realism and diagnostic utility, the adapter A_θ and classifier C_ϕ are jointly trained with:

$$\mathcal{L}_{\text{total}} = \underbrace{\mathcal{L}_{\text{recon}}(X_i, \hat{X}_i)}_{\text{Reconstruction}} + \lambda_{\text{cls}} \underbrace{\mathcal{L}_{\text{cls}}(y_i, \hat{y}_i)}_{\text{Classification}}. \quad (6)$$

The classification loss is cross-entropy, $\mathcal{L}_{cls} = \text{CE}(y_j, C_\phi(\hat{z}_j))$. Reconstruction combines L_1 , SSIM, and Total Variation (TV) [18]:

$$\mathcal{L}_{\text{recon}} = \|X_j - \hat{X}_j\|_1 + (1 - \text{SSIM}(X_j, \hat{X}_j)) + \lambda_{\text{TV}} \cdot \text{TV}(\hat{X}_j). \quad (7)$$

Joint optimization enables synthesis of structural MRIs preserving diagnostic biomarkers for patients without neuroimaging.

3 Experiments

Datasets and Preprocessing. We used data from 1,175 ADNI patients [8]. Each record includes 88-dimensional tabular EHR features, a structural brain MRI of $91 \times 109 \times 91$, and a binary label (Cognitively Normal [CN] or Alzheimer’s Disease [AD]). The cohort was randomly split into training and testing sets at a 7:3 ratio. To simulate real-world EHR-only scenarios, true MRIs of testing patients (\mathcal{P}_{te}) were masked during training. For the knowledge graph, we use iBKH [19] with over 2 million entities and 48 million triples. SapBERT [15] generates embeddings for patient-to-KG linking.

Baselines. We compare MIRAGE with: (1) EHR-only models (Logistic Regression, Random Forest, Multi-Layer Perceptron); (2) EHR→MRI conditional generation; (3) EHR→Latent MLP mapping to the AE space; (4) MVAE with shared latents; and (5) Conditional Diffusion with EHR-conditioned denoising.

Implementation Details. For MRI, volumes were skull-stripped via FSL-BET [9], registered to MNI152 space (1mm isotropic), and z-score normalized, yielding $182 \times 218 \times 182$ voxels. For downstream classification, a 3D CNN [12] is trained on real MRIs and evaluated on synthetic MRIs. We report Balanced Accuracy (BAcc), AUC, Sensitivity (SEN), and Specificity (SPE). To assess modality complementarity, we train a logistic regression fusion module. It takes a 3D vector $[p_{\text{EHR}}, p_{\text{MRI}}, |p_{\text{EHR}} - p_{\text{MRI}}|]$ as input, where p denotes probabilities from EHR baselines and the synthetic-MRI-based 3D CNN.

Main Results. Table 1 presents performance comparisons across all baselines. Unimodal EHR-only classifiers show limited prognostic capacity, indicating that tabular clinical records obscure critical neurodegenerative trajectories when processed in isolation. Standard generative baselines (Direct EHR→MRI, MVAE, and Conditional Diffusion) fail to produce clinically viable outputs, showing mode collapse, structural corruption, or extreme blurring. These failures reflect an information-theoretic limitation: synthesizing complex, high-frequency 3D anatomical structures de novo from low-dimensional tabular data without spatial priors violates the Data Processing Inequality. In contrast, MIRAGE circumvents this limitation by using the $K = 1$ nearest-neighbor skip features as an anatomical canvas, while the aligned latent embedding (\hat{z}_j) modulates disease-specific morphological changes. This biologically grounded synthesis generates

Table 1: Performance comparison across methods. Bold and underlined values indicate the best and second-best results, respectively. Upper-bound rows use real MRI and EHR+MRI inputs for reference only and are not directly comparable. Our method achieves the best balanced accuracy and sensitivity when combined with an MLP classifier, while remaining competitive across AUC and specificity.

Method	BAcc \uparrow	AUC \uparrow	SEN \uparrow	SPE \uparrow
MRI Upper Bound	0.81	0.85	0.84	0.77
EHR+MRI Upper Bound	0.73	0.62	0.71	0.75
Logistic Regression (LR)	0.66	0.75	0.58	0.75
Multi-Layer Perceptron (MLP)	0.62	0.72	0.42	0.82
Random Forest (RF)	0.67	0.80	0.39	0.86
EHR \rightarrow MRI	0.65	0.72	0.52	0.80
EHR-latent-decoder	0.64	0.72	0.48	0.81
MVAE	0.67	0.71	0.50	0.84
Conditional Diffusion	0.66	0.67	0.47	<u>0.84</u>
Ours (LR+Syn MRI)	0.67	0.75	<u>0.56</u>	0.78
Ours (MLP+Syn MRI)	0.70	0.75	0.63	0.78
Ours (RF+Syn MRI)	<u>0.68</u>	<u>0.78</u>	0.55	0.81

clear, anatomically coherent MRIs that preserve individualized neurodegenerative biomarkers. When evaluated with a downstream 3D CNN, the reconstructed MRIs consistently amplify the prognostic value of the original EHR data. The MIRAGE-augmented fusion protocol improves the classification rate by 13% over the strongest EHR-only baseline, showing that projecting clinical phenotypes into a structural manifold unlocks hidden diagnostic signals.

Ablation Studies. To isolate the contribution of each module and verify that the framework synthesizes patient-specific pathology rather than replicating cohort neighbors, we analyze four ablation settings (Table 2). The strong performance degradation in the *w/o KG* (direct EHR-to-latent MLP) and *w/o GAT* (nearest-neighbor feature transfer) settings validates that structured ontological mapping and dynamic message passing are essential for mitigating EHR sparsity and noise. Furthermore, the *w/o AE* ablation, replacing the AE manifold with an MLP generator, causes performance collapse and confirms that a pre-trained population-level structural manifold is required to prevent generative hallucination. The decline in the *w/o Adapter* setting (direct GAT-to-decoder decoding) highlights the need for the cross-modal alignment layer to bridge graph-structured clinical priors and latent image representations. The *w/o Adapter* ablation also provides evidence against nearest-neighbor feature copying. In this setting, the decoder receives raw graph-propagated embeddings and $K = 1$ spatial skip features. If the downstream 3D CNN relied on anatomical structures from clinical neighbors via skip connections, the performance drop would be marginal. Instead, diagnostic accuracy declines sharply when the adapter is removed. This confirms that high-frequency skip features provide non-diagnostic structural background, while disease-specific biomarkers such as ventricular expansion and hippocampal atrophy are synthesized from the aligned latent vector.

Case Study and Human Evaluation. To evaluate the clinical fidelity of synthesized MRIs, we conducted a human assessment with two biomedical ex-

Table 2: Ablation study results.

	BAcc	AUC	SEN	SPE
Ours	0.70	0.75	0.63	0.78
w/o KG	0.54	0.56	0.27	0.81
w/o GAT	0.58	0.58	0.44	0.72
w/o AE	0.61	0.64	0.47	0.76
w/o Adapter	0.58	0.54	0.42	0.73

Table 3: Human evaluation results.

Metric	Real Synth.	
Anat. Real.	0.54	0.42
Clin. Usab.	3.04	2.96
Diag. Interp.	3.00	2.98

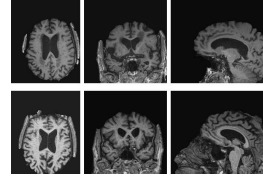


Fig. 2: Case studies.

perts. We randomly sampled 50 scans (25 real, 25 synthetic) and evaluated three dimensions: (i) Anatomical Realism (binary Yes/No rate); (ii) Clinical Usability (5-point visual quality scale); and (iii) Diagnostic Interpretability (5-point structural clarity scale). As shown in Table 3, MIRAGE achieves high parity with real MRIs, with synthetic scans nearly indistinguishable from ground truth anatomically. The specialists confirmed that synthetic MRIs consistently exhibit AD-related biomarkers, including hippocampal atrophy and ventricular enlargement, aligned with clinical profiles. This validation shows that the framework not only generates realistic images but also translates EHR-based disease patterns into clinically valid structural evidence for downstream diagnostic support.

4 Discussion

The experimental results show that MIRAGE bridges the modality gap in AD diagnosis by synthesizing anatomically and clinically consistent MRIs from heterogeneous EHR data. Rather than a traditional feature engineering tool, the framework uses MRI synthesis as a generative objective forcing the model to distill high-dimensional clinical narratives into biologically grounded structural evidence. This process, termed generative feature distillation, leverages reconstruction of realistic brain anatomy, such as hippocampal volume or cortical thickness, to constrain the latent space and prioritize diagnostically useful features. Central to this success is the Biomedical Knowledge Graph (KG) as a semantic anchor, bypassing inconsistent EHR schemas by linking patients through standardized clinical entities. This ensures latent factors of neurodegeneration remain stable across cohorts, enabling transfer of imaging priors to EHR-only patients. By translating unstructured clinical observations into radiological evidence, MIRAGE improves predictive performance and interpretability via pathologically relevant biomarkers. Nevertheless, the study is limited by a lack of evaluation on external cohorts beyond ADNI. Although results show strong internal validity, future work will validate the framework on independent real-world EHR-only cohorts to assess generalization and robustness across clinical settings.

5 Conclusion

In this work, we introduced MIRAGE, a knowledge graph-guided cross-modal MRI synthesis framework designed to generate anatomically realistic and clinically meaningful MRIs for patients with only EHR data. By integrating 3D MRI autoencoding, knowledge graph-based embedding propagation, and adapter-decoder alignment, MIRAGE enables structure-consistent MRI generation without paired EHR-MRI training data. Experiments demonstrate that the synthesized MRIs preserve disease-relevant anatomy and enhance AD classification. Future work will extend MIRAGE to broader datasets and modalities to further assess its generalizability across clinical cohorts.

References

1. Barker, W.W., Luis, C.A., Kashuba, A., Luis, M., Harwood, D.G., Loewenstein, D., Waters, C., Jimison, P., Shepherd, E., Sevush, S., et al.: Relative frequencies of alzheimer disease, lewy body, vascular and frontotemporal dementia, and hippocampal sclerosis in the state of florida brain bank. *Alzheimer Disease & Associated Disorders* **16**(4), 203–212 (2002)
2. Brody, S., Alon, U., Yahav, E.: How attentive are graph attention networks? arXiv preprint arXiv:2105.14491 (2021)
3. Duenias, D., Nichyporuk, B., Arbel, T., Raviv, T.R., et al.: Hyperfusion: A hyper-network approach to multimodal integration of tabular and medical imaging data for predictive modeling. *Medical Image Analysis* **102**, 103503 (2025)
4. Edelstein, W.A., Mahesh, M., Carrino, J.A.: Mri: time is dose—and money and versatility. *Journal of the American College of Radiology: JACR* **7**(8), 650 (2010)
5. Frisoni, G.B., Hansson, O., Nichols, E., Garibotto, V., Schindler, S.E., van der Flier, W.M., Jessen, F., Villain, N., Arenaza-Urquijo, E.M., Crivelli, L., et al.: New landscape of the diagnosis of alzheimer’s disease. *The Lancet* **406**(10510), 1389–1407 (2025)
6. Fu, M., Sankararaman, S., Pasaniuc, B., Vessel, K., Chang, T.S.: Identifying common disease trajectories of alzheimer’s disease with electronic health records. *EBioMedicine* **118** (2025)
7. Huang, S.C., Pareek, A., Seyyedi, S., Banerjee, I., Lungren, M.P.: Fusion of medical imaging and electronic health records using deep learning: a systematic review and implementation guidelines. *NPJ digital medicine* **3**(1), 136 (2020)
8. Jack Jr, C.R., Bernstein, M.A., Fox, N.C., Thompson, P., Alexander, G., Harvey, D., Borowski, B., Britson, P.J., L. Whitwell, J., Ward, C., et al.: The alzheimer’s disease neuroimaging initiative (adni): Mri methods. *Journal of Magnetic Resonance Imaging: An Official Journal of the International Society for Magnetic Resonance in Medicine* **27**(4), 685–691 (2008)
9. Jenkinson, M., Beckmann, C.F., Behrens, T.E., Woolrich, M.W., Smith, S.M.: Fsl. *Neuroimage* **62**(2), 782–790 (2012)
10. Jiang, P., Xiao, C., Cross, A., Sun, J.: Graphcare: Enhancing healthcare predictions with personalized knowledge graphs. arXiv preprint arXiv:2305.12788 (2023)
11. Le, L.P., Nguyen, T., Riegler, M.A., Halvorsen, P., Nguyen, B.T.: Multimodal missing data in healthcare: A comprehensive review and future directions. *Computer Science Review* **56**, 100720 (2025)

12. Li, S., Zhang, Y., Zou, C., Zhang, L., Li, F., Liu, Q.: Transformer attention-based neural network for cognitive score estimation from smri data. *Computers in Biology and Medicine* **196**, 110579 (2025)
13. Li, Y., Fang, C., Yang, J., Wang, Z., Lu, X., Yang, M.H.: Universal style transfer via feature transforms. *Advances in neural information processing systems* **30** (2017)
14. Lin, D.J., Doshi, A.M., Fritz, J., Recht, M.P.: Designing clinical mri for enhanced workflow and value. *Journal of Magnetic Resonance Imaging* **60**(1), 29–39 (2024)
15. Liu, F., Shareghi, E., Meng, Z., Basaldella, M., Collier, N.: Self-alignment pretraining for biomedical entity representations. In: *Proceedings of the 2021 conference of the North American chapter of the association for computational linguistics: human language technologies*. pp. 4228–4238 (2021)
16. Liu, W., Fan, S., Weng, G.: Multi-modal deep learning framework for early alzheimer’s disease detection using mri neuroimaging and clinical data fusion. *Annals of Applied Sciences* **6**(1) (2025)
17. Qiu, S., Miller, M.I., Joshi, P.S., Lee, J.C., Xue, C., Ni, Y., Wang, Y., De Anda-Duran, I., Hwang, P.H., Cramer, J.A., et al.: Multimodal deep learning for alzheimer’s disease dementia assessment. *Nature communications* **13**(1), 3404 (2022)
18. Rudin, L.I., Osher, S., Fatemi, E.: Nonlinear total variation based noise removal algorithms. *Physica D: nonlinear phenomena* **60**(1-4), 259–268 (1992)
19. Su, C., Hou, Y., Zhou, M., Rajendran, S., Maasch, J.R., Abedi, Z., Zhang, H., Bai, Z., Cuturrufo, A., Guo, W., et al.: Biomedical discovery through the integrative biomedical knowledge hub (ibkh). *Iscience* **26**(4) (2023)
20. Veličković, P., Cucurull, G., Casanova, A., Romero, A., Lio, P., Bengio, Y.: Graph attention networks. *arXiv preprint arXiv:1710.10903* (2017)
21. Wang, S., Lin, M., Ghosal, T., Ding, Y., Peng, Y.: Knowledge graph applications in medical imaging analysis: a scoping review. *Health data science* **2022**, 9841548 (2022)
22. Wang, Z., Bovik, A.C., Sheikh, H.R., Simoncelli, E.P.: Image quality assessment: from error visibility to structural similarity. *IEEE transactions on image processing* **13**(4), 600–612 (2004)
23. Wu, G., Xie, Y., Wu, H., He, Z., Shao, H., Hu, X., Yang, C.: Utilizing large language models for zero-shot medical ontology extension from clinical notes. *arXiv preprint arXiv:2511.16548* (2025)
24. Xie, Y., Han, X., Xu, R., Hu, X., Lu, J., Yang, C.: Hypkg: Hypergraph-based knowledge graph contextualization for precision healthcare. In: *International Semantic Web Conference*. pp. 328–348. Springer (2025)
25. Xie, Y., Lu, J., Ho, J., Nahab, F., Hu, X., Yang, C.: Promptlink: leveraging large language models for cross-source biomedical concept linking. In: *Proceedings of the 47th International ACM SIGIR Conference on Research and Development in Information Retrieval*. pp. 2589–2593 (2024)
26. Xie, Y., Niu, G., Da, Q., Dai, W., Yang, Y.: Survival prediction for gastric cancer via multimodal learning of whole slide images and gene expression. In: *2022 IEEE international conference on bioinformatics and biomedicine (BIBM)*. pp. 1311–1316. IEEE (2022)
27. Zhang, C., Chu, X., Ma, L., Zhu, Y., Wang, Y., Wang, J., Zhao, J.: M3care: Learning with missing modalities in multimodal healthcare data. In: *Proceedings of the 28th ACM SIGKDD conference on knowledge discovery and data mining*. pp. 2418–2428 (2022)

28. Zhang, Z., Cui, H., Xu, R., Xie, Y., Ho, J.C., Yang, C.: Tacco: Task-guided co-clustering of clinical concepts and patient visits for disease subtyping based on ehr data. In: Proceedings of the 30th ACM SIGKDD Conference on Knowledge Discovery and Data Mining. pp. 6324–6334 (2024)
29. Zhu, L., Xue, Z., Jin, Z., Liu, X., He, J., Liu, Z., Yu, L.: Make-a-volume: Leveraging latent diffusion models for cross-modality 3d brain mri synthesis. In: International Conference on Medical Image Computing and Computer-Assisted Intervention. pp. 592–601. Springer (2023)